iScience, Volume *24*

Supplemental Information

Coproduction of hydrogen and lactic acid from glucose photocatalysis on band-engineered $Zn_{1-x}Cd_xS$ homojunction

Heng Zhao, Chao-Fan Li, Xue Yong, Pawan Kumar, Bruna Palma, Zhi-Yi Hu, Gustaaf Van Tendeloo, Samira Siahrostami, Stephen Larter, Dewen Zheng, Shanyu Wang, Zhangxin Chen, Md Golam Kibria, and Jinguang Hu

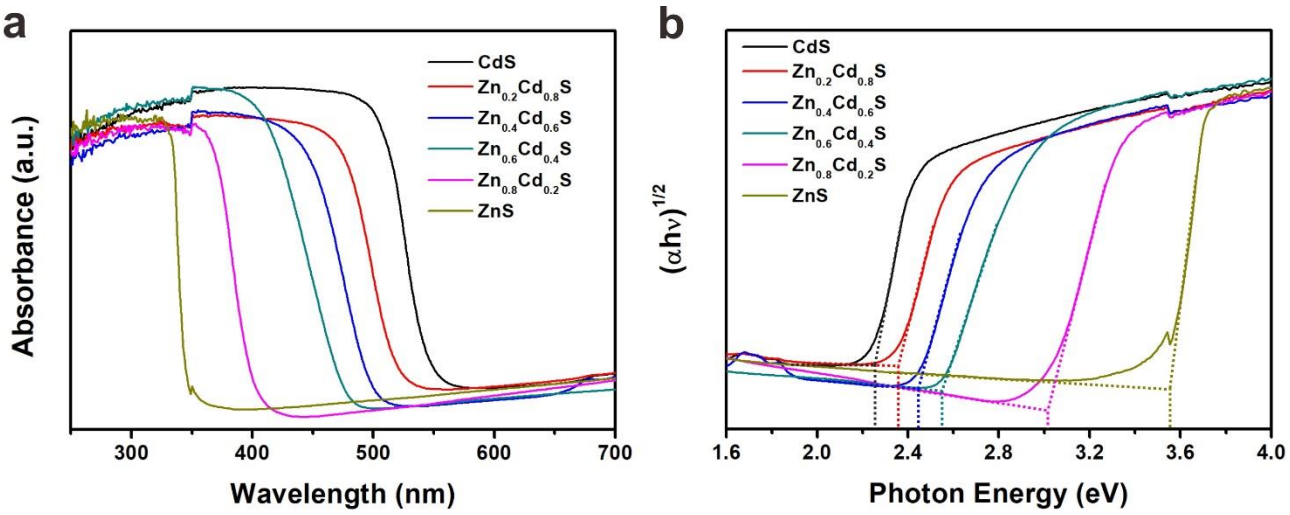

Figure S1 Optical properties (Related to Figure 1). (a) UV-vis diffuse reflectance spectra and (b) corresponding Tauc plot of $Zn_{1-x}Cd_xS$ solid solutions with different x values.

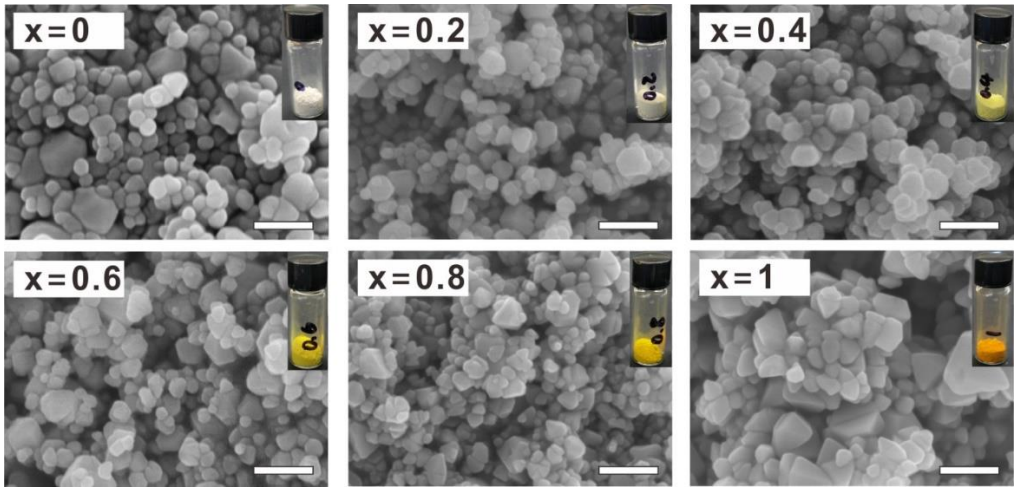

Figure S2 Mophology characterization (Related to Figure 2). SEM images and photographs of $Zn_{1-x}Cd_xS$ solid solutions with different x values (scale bar: 200 nm).

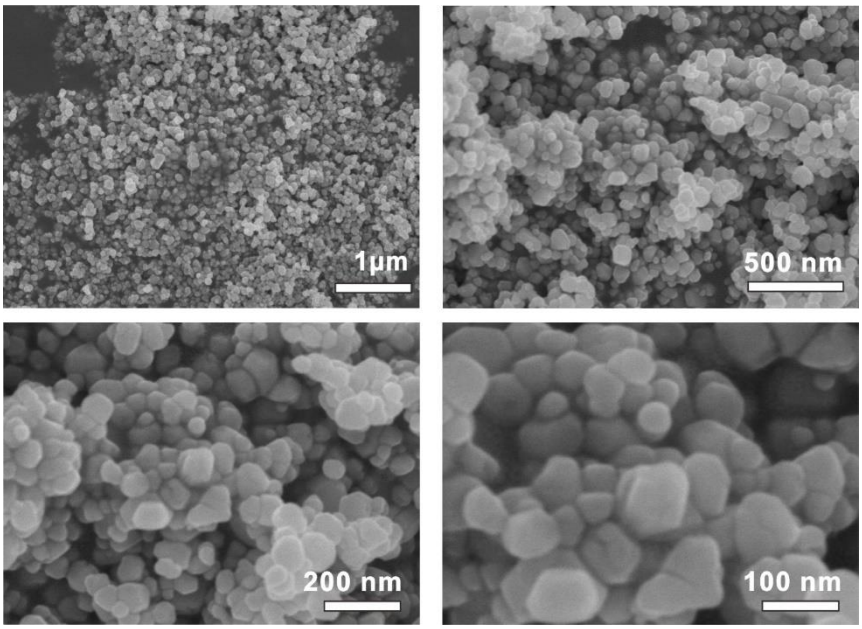

Figure S3 Mophology characterization (Related to Figure 2). SEM images of $Zn_{0.6}Cd_{0.4}S$ with different resolutions.

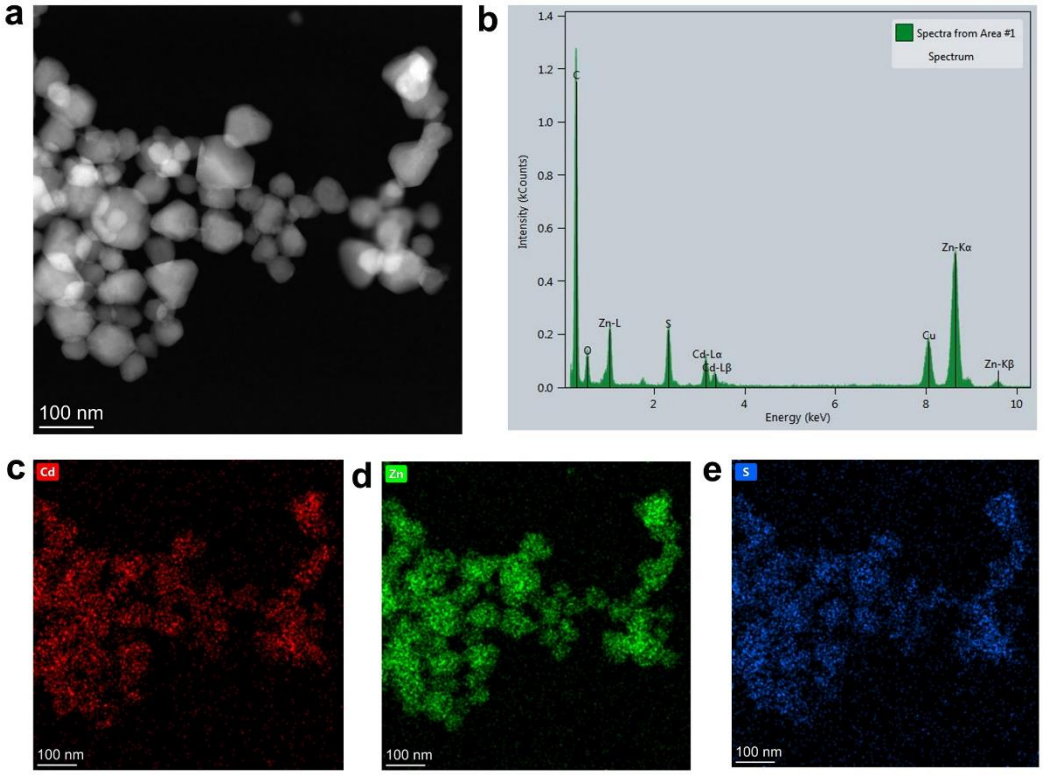

Figure S4 Mophology characterization (Related to Figure 2). (a) HAADF-STEM image at low magnification, (b) EDS spectrum of the whole area in (a), (c-e) EDS elemental maps: Cd (red), Zn (green) and S (blue) for $Zn_{0.6}Cd_{0.4}S$.

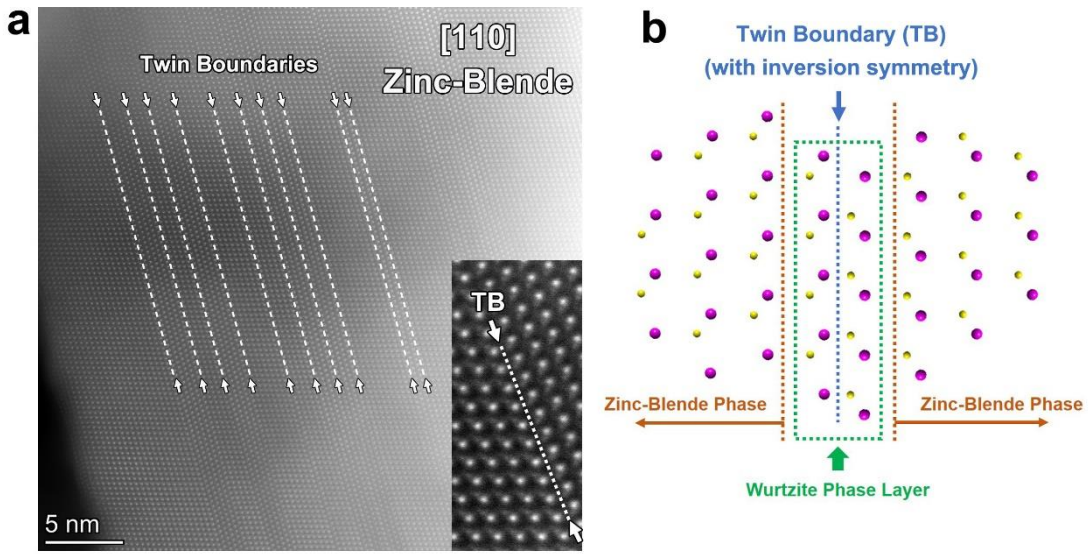

Figure S5 Structural characterization and schematic illustration of homojunction (Related to Figure 2). (a) HR-HAADF-STEM image of a zinc-blende particle and corresponding enlarged HAADF-STEM image of a twin boundary, (b) the model of twin boundary with inversion symmetry.

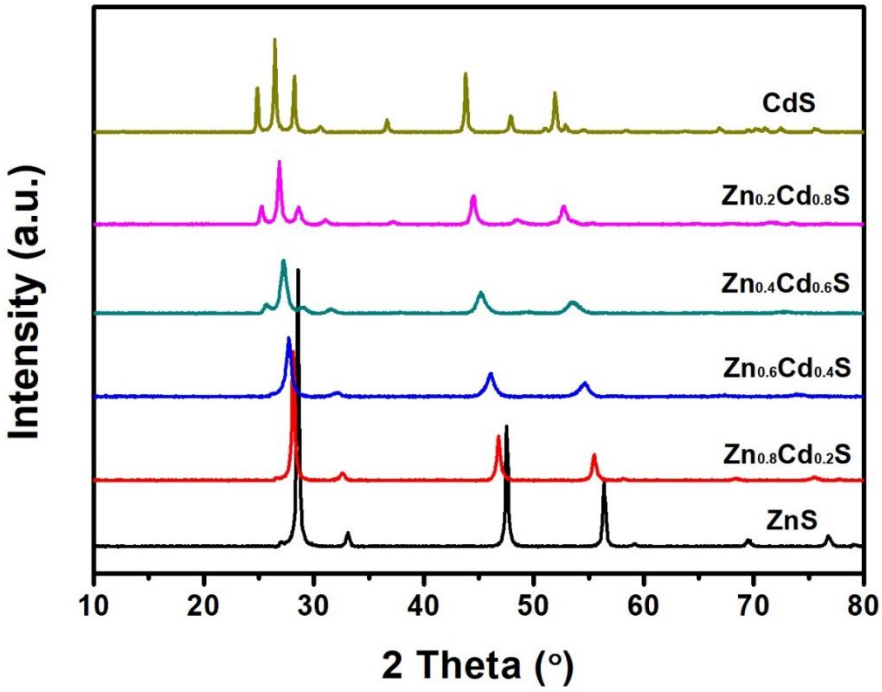

Figure S6 Crystal structure characterization (Related to Figure 2). XRD patterns of $Zn_{1-x}Cd_xS$ solid solutions.

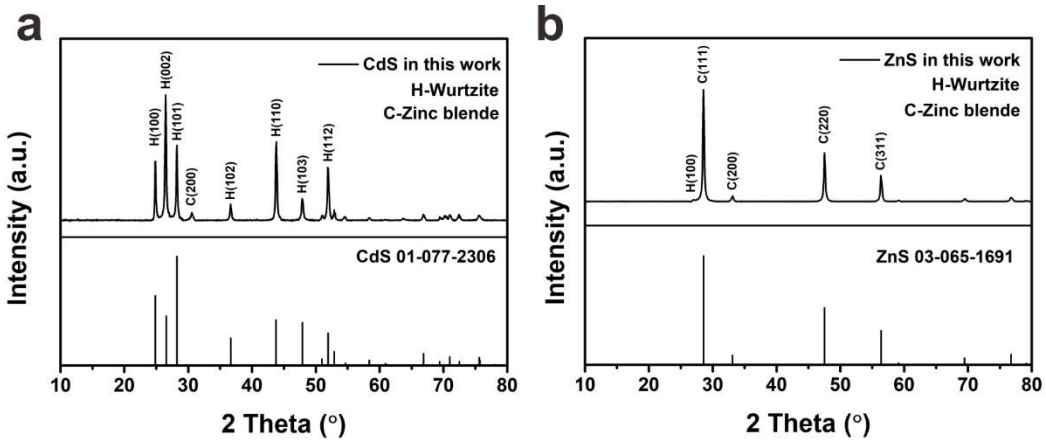

Figure S7 Crystal structure characterization (Related to Figure 2). XRD and standard patterns from JCPDS Card for CdS and ZnS.

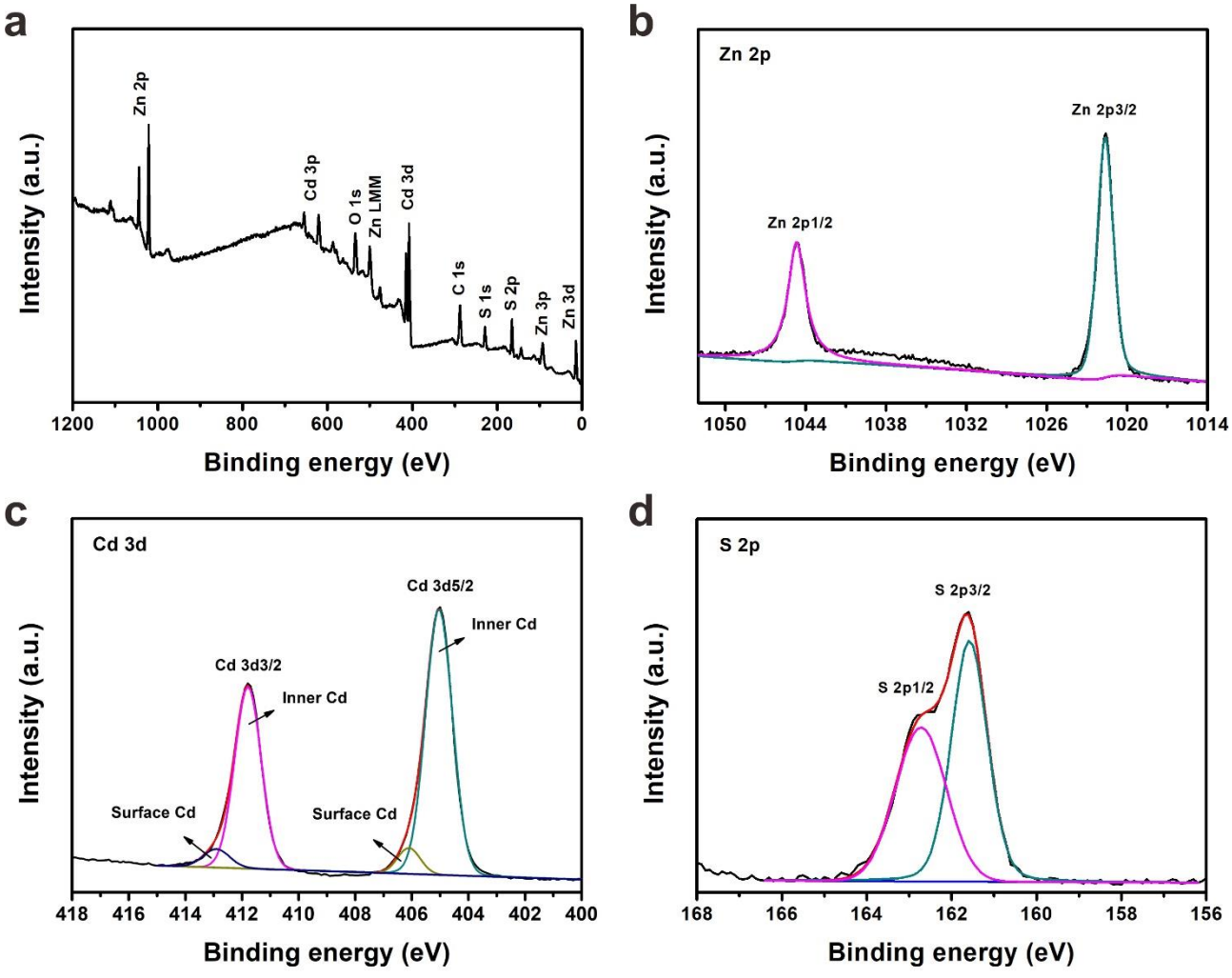

Figure S8 Component and chemical states (Related to Figure 2). (a) XPS survey spectrum and (b) Zn 2p, (c) Cd 3d and (d) S 2p spectra of $Zn_{0.6}Cd_{0.4}S$.

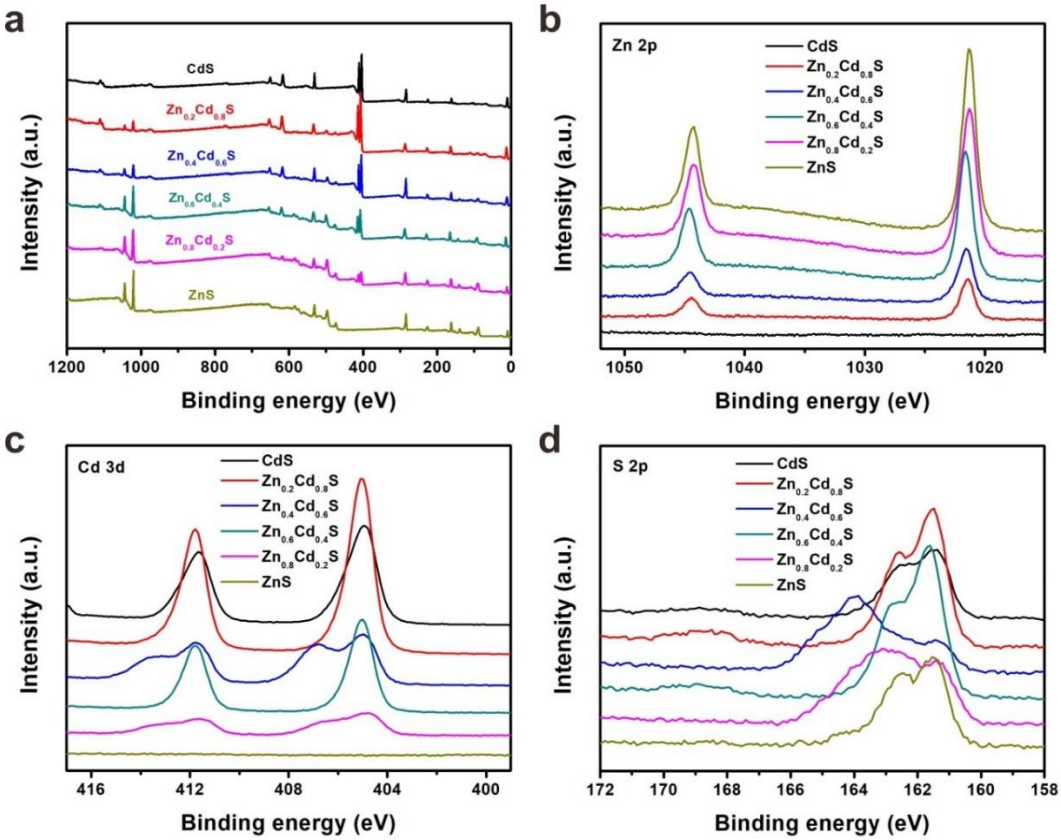

Figure S9 Component and chemical states (Related to Figure 2). (a) XPS survey spectra and high-resolution XPS spectra of (b) Zn 2p, (c) Cd 3d and (d) S 2p for $Zn_{1-x}Cd_xS$ solid solutions with different x values.

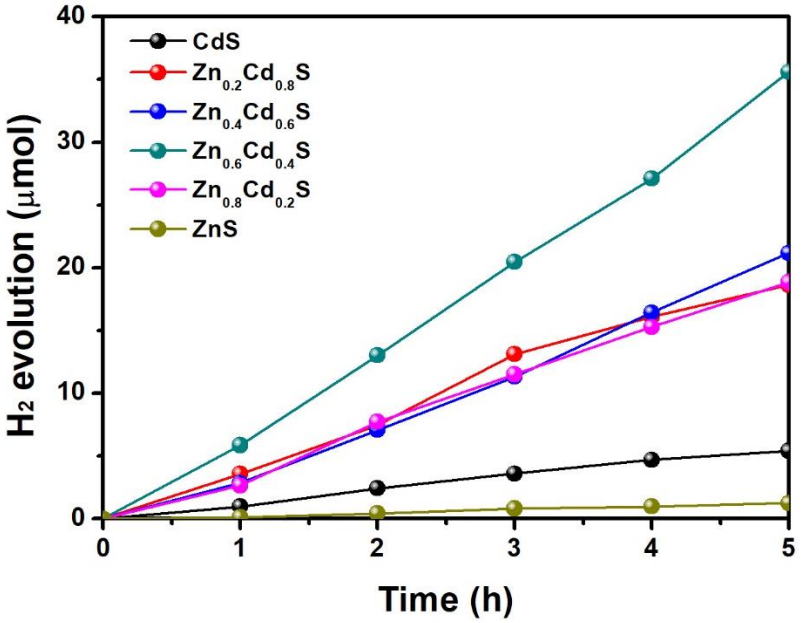

Figure S10 Hydrogen production (Related to Figure 3). (a) Photocatalytic hydrogen evolution activities of $Zn_{1-x}Cd_xS$ solid solutions in 20 g/L glucose solution.

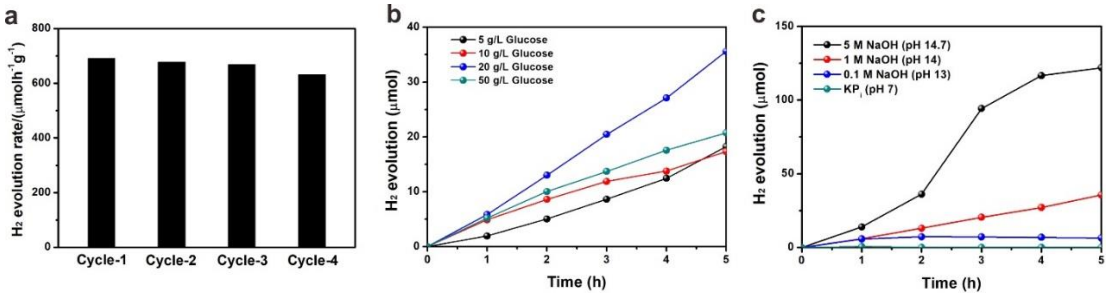

Figure S11 Hydrogen production (Related to Figure 3). (a) Photocatalytic stability of $Zn_{0.6}Cd_{0.4}S$ in four cycles and each cycle is 5 h. (b) Photocatalytic hydrogen performance of $Zn_{0.6}Cd_{0.4}S$ in different glucose concentrations. (c) Photocatalytic hydrogen performance of $Zn_{0.6}Cd_{0.4}S$ in different alkali concentration (pH).

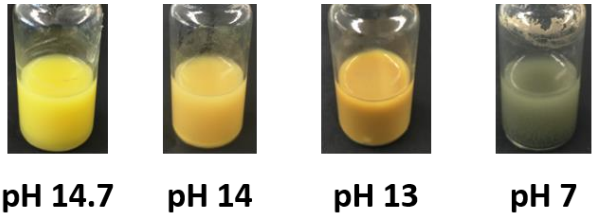

Figure S12 Photocorrosion (Related to Figure 3). Photographs of the solutions after reaction in different alkali concentration.

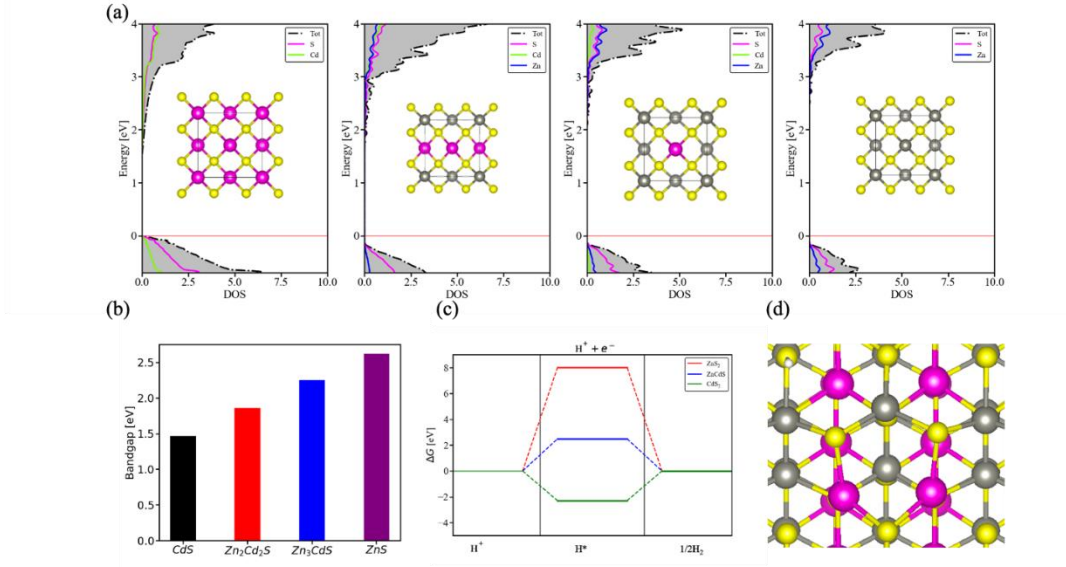

Figure S13 Structural simulation and bandgap calculation (Related to Figure 3). (a) The density of states for CdS, $Zn_{0.5}Cd_{0.5}S$, $Zn_{0.75}CdS$, ZnS (b) the band gaps for (c) The calculated = free-energy diagram of HER at the equilibrium potential for CdS, $Zn_{0.5}Cd_{0.5}S$, and ZnS. (d) The lowest energy model structure of H absorbed on $Zn_{0.5}Cd_{0.5}S$.

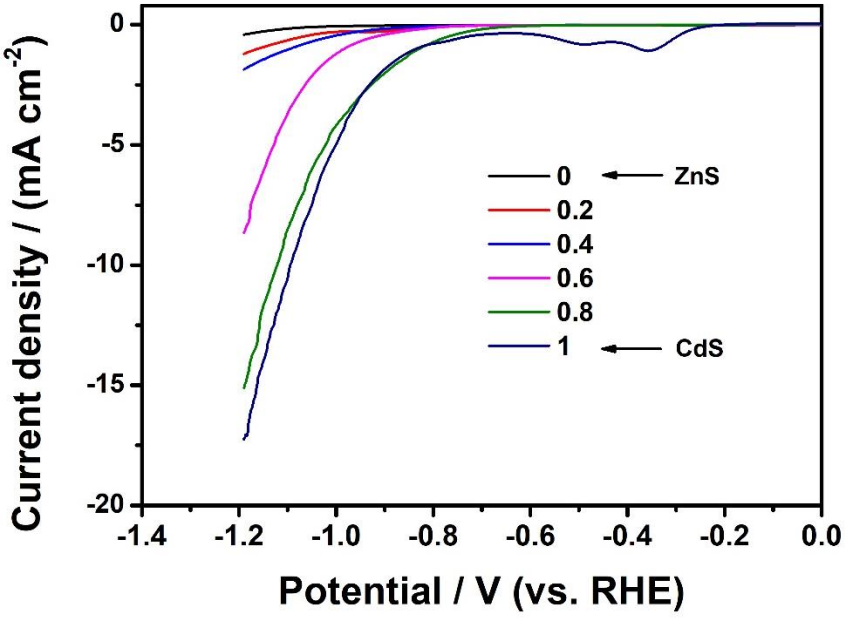

Figure S14 Electrochemical test (Related to Figure 3). Polarization curves of $Zn_{1-x}Cd_xS$ solid solutions with different x values. Condition: Pt/C with catalyst as the working electrode, Pt wire as the counter electrode and Ag/AgCl as the reference electrode, 1.0 M KOH as electrolyte. The working electrode was obtained by dip-coating 40 μL photocatalyst slurry (20 mg sample and 50 μL of 5 wt % Nafion solution were dispersed in 1 mL of 3:1 v/v water/isopropanol mixed solvent) onto the prewashed Pt/C electrode.

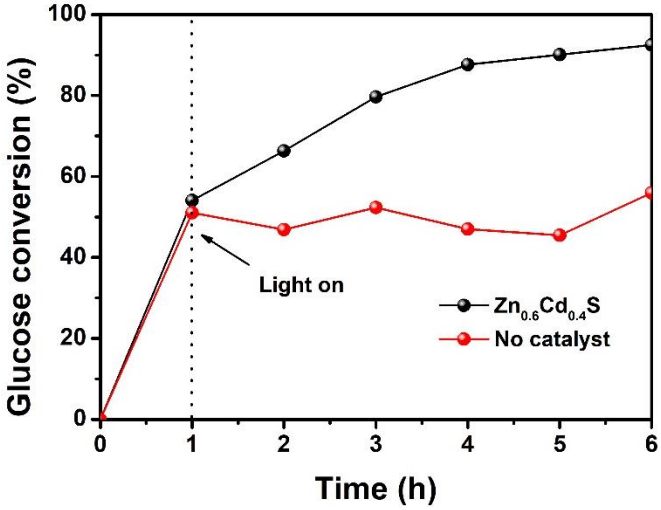

Figure S15 Glucose conversion (Related to Figure 4). Glucose conversion along with reaction time with and without photocatalyst. Reaction conditions: 10 mg photocatalyst, 5 mL 20 g/L glucose in 1 M NaOH, vacuum condition, Xenon lamp (λ = 400-780 nm), room temperature.

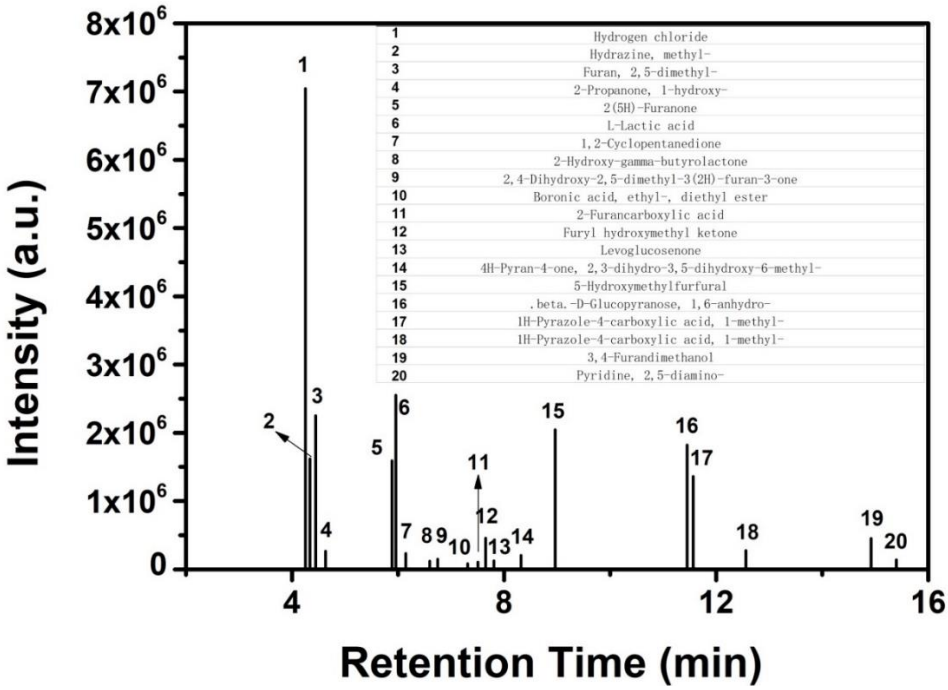

Figure S16 Products analysis (Related to Figure 4). GC-MS signals for the products in liquid after photocatalytic reaction and the matched products according to the database.

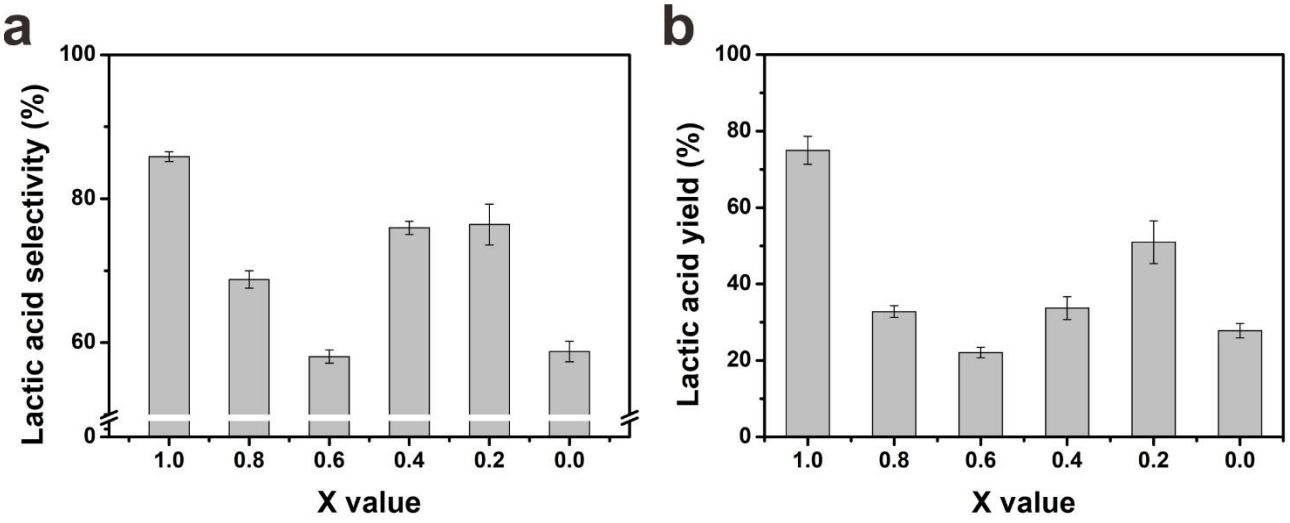

Figure S17 Lactic acid production (Related to Figure 4). Lactic acid selectivity and yield of $Zn_{1-x}Cd_xS$ solid solutions with different x values.

The glucose conversion, selectivity and yield of lactic acid were calculated using the following formulas:

Glucose conversion (%) = $((Glucose)_{in}-(Glucose)_{out})/ (Glucose)_{in}$

Lactic acid selectivity (%) = $(Lactic\ acid)_{out}/((Lactic\ acid)_{out} + (Formic\ acid)_{out} + (Fructose)_{out})$

Lactic acid yield (%) = Carbon of lactic acid / Carbon of converted glucose

Selectivity and yield values were calculated on a molar basis.

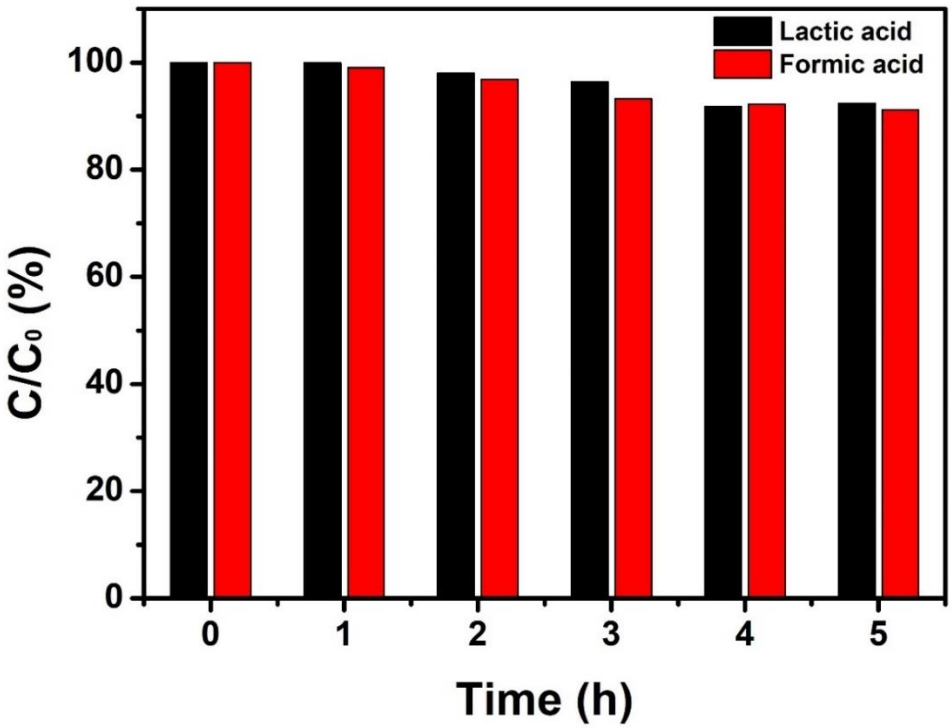

Figure S18 Stability of lactic acid and formic acid during the reaction (Related to Figure 4). Lactic acid and formic acid conversion over $Zn_{0.6}Cd_{0.4}S$. Reaction conditions: 10 mg photocatalyst, 5 mL 20 g/L lactic acid or formic acid in 1 M NaOH, vacuum condition, Xenon lamp (λ = 400-780 nm), room temperature.

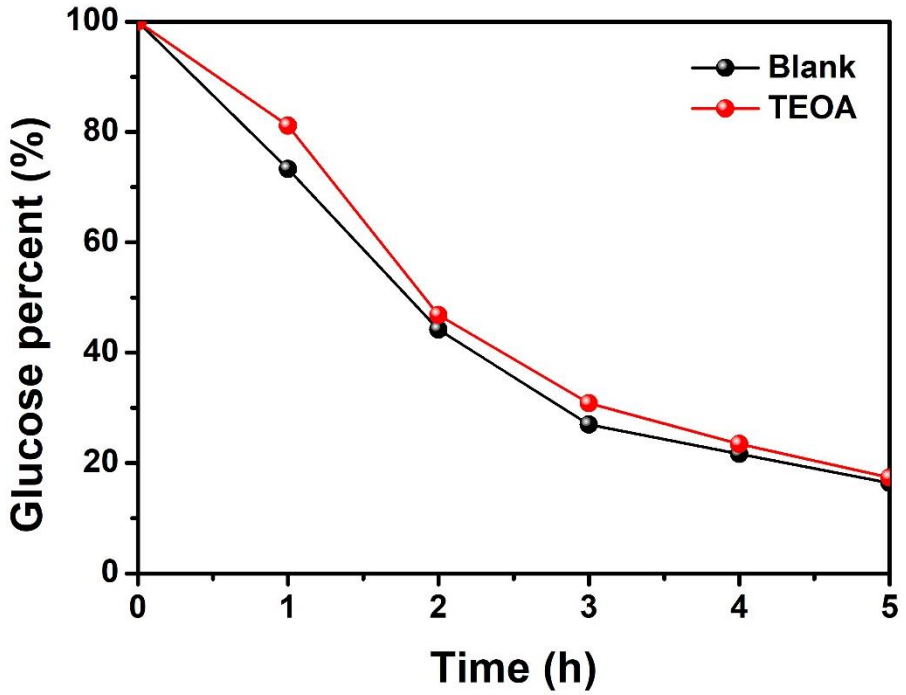

Figure S19 Scavenger test (Related to Figure 5). Glucose conversions without any sacrificial agent and in presence of TEOA over $Zn_{0.6}Cd_{0.4}S$.

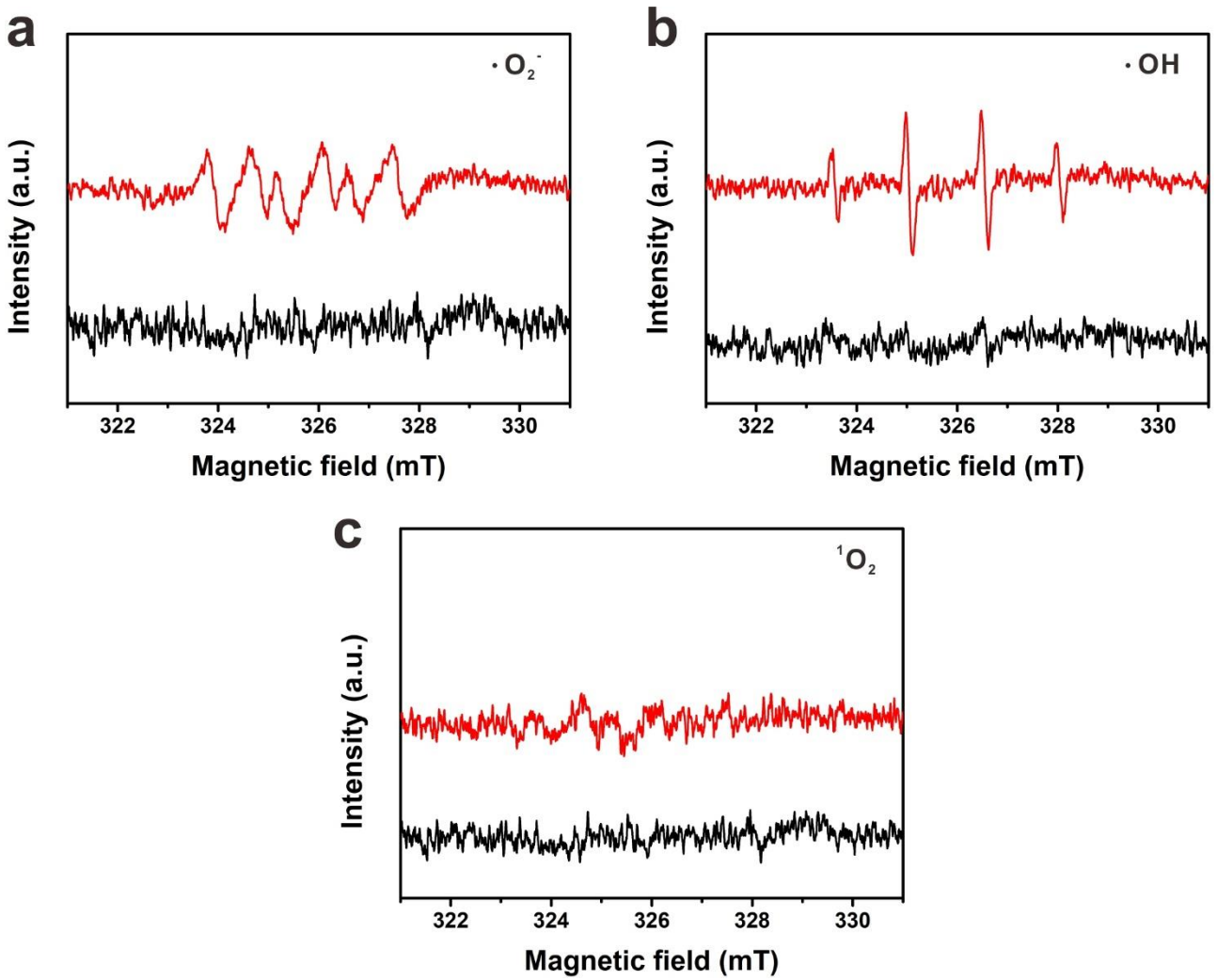

Figure S20 Active oxygen species (Related to Figure 5). DMPO ESR spin-trapping for (a) $\cdot O_2^-$ and (b) ·OH, TEMPONE ESR spin-trapping for (c) $^1O_2$ over $Zn_{0.6}Cd_{0.4}S$ (black line: under dark condition and red line: with light irradiation).

Transparent Methods

Materials

All the reagents in this experiment were of analytical grade and commercially available. Zinc acetate dihydrate ($Zn(CH_3COO)_2 \cdot 2H_2O$, 98.0%), cadmium acetate dihydrate ($Cd(CH_3COO)_2 \cdot 2H_2O$, 98.0%), thioacetamide (TAA, 99.0%), 1-octanol (99.0%), ethylene glycol (EG, 99.8%) and ethanol were purchased from Millipore Sigma.

Synthesis of $Zn_{1-x}Cd_xS$ solid solution

In typical, 8 mmol TAA was dissolved in a mixed solution containing 20 mL EG, 10 mL 1-octanol and 10 mL water. Then, a total 4 mmol of $Zn(CH_3COO)_2 \cdot 2H_2O$ and $Cd(CH_3COO)_2 \cdot 2H_2O$ with the desired atomic ratio was added into the above solution. The obtained aqueous solution was transferred to a 50 mL Teflon-lined stainless-steel autoclave after 30 min of continuous stirring and heated at 180 ℃ for 4 h. The resulting precipitate was collected after centrifugation, washed with ethanol three times and dried in an oven at 80 ℃ overnight. A series of $Zn_{1-x}Cd_xS$ solid solutions with x values of 0, 0.2, 0.4, 0.6, 8 and 1 can be prepared by changing the molar ratio between $Zn(CH_3COO)_2 \cdot 2H_2O$ and $Cd(CH_3COO)_2 \cdot 2H_2O$.

Characterization

The crystalline phase in the samples was examined by powder X-ray diffraction (XRD, D8 ADVANCE) equipped with a Cu anode X-ray tube (Cu Kα X-rays, λ=1.54056 Å). The rough surface morphology of the samples was observed with a field-emission scanning electron microscope (SEM, Hitachi S-4800). The local structure of the materials has been determined using a double aberration corrected transmission electron microscope (TEM, Thermo Fisher Titan Themis) equipped with a Super-X energy dispersive X-ray detector (EDX) at 300 keV. X-ray photoelectron spectroscopy (XPS) to determine the surface chemical composition and binding energy of constituting elements were recorded on a customized X-ray photoelectron spectrometer (Kratos AXIS Ultra DLD equipped with a monochromatic Al Kα source). All the raw data was calibrated using the C (1s) peak of adventitious carbons at a binding energy 284.8 eV. The UV-vis absorption spectra were recorded in a diffuse reflectance mode on a SHIMADZU UV-Vis spectrophotometer with an integrating sphere scanning in a spectral range of 300-800 nm. The Brunauer-Emmett-Teller (BET) specific surface areas of the powders were determined using N_2 adsorption-desorption isotherms at 77 K on a Gemini

VII (Micromeritics Corp.). The zeta potential was measured using the Nanoplus zeta analyzer (Nano-ZS, Malvern).

Photocatalytic glucose conversion

Typically, the photocatalytic testing was performed in closed glass vials (12 mL) at room temperature using a 300 W Xenon lamp (Excelitas Tech.). 10 mg photocatalyst was dispersed in a mixed solution of 20 g/L substrate and 5 mL NaOH (1 M) solution. The closed glass vial containing the above mixture was sonicated and degassed for 0.5 h and finally irradiated under AM1.5 G solar simulated light. The evolved H_2 was periodically quantified by using gas chromatography (GC, PerkinElmer Clarus 590) equipped with a Molecular Sieve 5A packed column and a thermal conductivity detector (TCD). The glucose stock solutions (for calibration) and reaction products were analyzed by using a 1200 HPLC Agilent system equipped with a refractive index detector (RID) and a photodiode array detector (DAD). The column was Hi-Plex H (6.5 × 300 mm, 8 μm, Agilent) and 0.005 M H_2SO_4 was used as an eluting solvent with a flow rate of 0.5 mL/min. Each experiment was repeated for three time to have the error bar.